Asymmetric segregation and self-renewal of hematopoietic stem and progenitor cells with endocytic Ap2a2

Stephen B. Ting,[1-3] Eric Deneault,[1] Kristin Hope,[1] Sonia Cellot,[1,4] Jalila Chagraoui,[1] Nadine Mayotte,[1] Jonas F. Dorn,[5] Jean-Philippe Laverdure,[1] Michael Harvey,[2] Edwin D. Hawkins,[2] Sarah M. Russell,[2,6] Paul S. Maddox,[5] Norman N. Iscove,[7] and Guy Sauvageau[1,8]

[1]Molecular Genetics of Stem Cells Laboratory, Institute of Research in Immunology and Cancer (IRIC), University of Montreal, Montreal, QC; [2]Immune Signalling Laboratory, Cancer Immunology, Research Division, Peter MacCallum Cancer Centre, East Melbourne, Australia; [3]Department of Clinical Hematology, Peter MacCallum Cancer Centre, East Melbourne, Australia; [4]Hematology and Oncology and Division of Viral and Immune Disorders and Cancers, Centre Hospitalier Universitaire Sainte-Justine, Montreal, QC; [5]Mitotic Mechanisms and Chromosome Dynamics Laboratory, IRIC, University of Montreal, Montreal, QC; [6]Centre for Micro-Photonics, Faculty of Engineering and Industrial Sciences, Swinburne University of Technology, Hawthorn, Australia; [7]Department of Medical Biophysics and Immunology, The Ontario Cancer Institute, University of Toronto, Toronto, ON; and [8]Division of Hematology and Leukemia Cell Bank of Quebec, Maisonneuve-Rosemont Hospital, Montreal, QC

The stem cell–intrinsic model of self-renewal via asymmetric cell division (ACD) posits that fate determinants be partitioned unequally between daughter cells to either activate or suppress the stemness state. ACD is a purported mechanism by which hematopoietic stem cells (HSCs) self-renew, but definitive evidence for this cellular process remains open to conjecture. To address this issue, we chose 73 candidate genes that function within the cell polarity network to identify potential determinants that may concomitantly alter HSC fate while also exhibiting asymmetric segregation at cell division. Initial gene-expression profiles of polarity candidates showed high and differential expression in both HSCs and leukemia stem cells. Altered HSC fate was assessed by our established in vitro to in vivo screen on a subcohort of candidate polarity genes, which revealed 6 novel positive regulators of HSC function: *Ap2a2*, *Gpsm2*, *Tmod1*, *Kif3a*, *Racgap1*, and *Ccnb1*. Interestingly, live-cell videomicroscopy of the endocytic protein AP2A2 shows instances of asymmetric segregation during HSC/progenitor cell cytokinesis. These results contribute further evidence that ACD is functional in HSC self-renewal, suggest a role for *Ap2a2* in HSC activity, and provide a unique opportunity to prospectively analyze progeny from HSC asymmetric divisions. (*Blood*. 2012; 119(11):2510-2522)

Introduction

Self-renewal is inextricably linked to stem cell division, and despite the premise that these processes in mammalian systems likely involve asymmetric cell division (ACD), the molecular details remain enigmatic. Our approach to addressing self-renewal via ACD in the hematopoietic stem cell (HSC) is based on increasing evidence that the mechanistic insights pertaining to polarity molecular networks, which are integral to ACD and cell fate in the invertebrate models of *Drosophila melanogaster* and *Caenorhabditis elegans*, are functionally conserved throughout evolution.[1-3]

Studies from invertebrate models support both extrinsic (niche) and stem cell–intrinsic mechanisms of ACD. In relation to the cell intrinsic machinery, polarity is initiated by asymmetrically localizing protein complexes to the cell membrane. Subcomponents of these complexes act as cell fate determinants that are maintained asymmetrically during mitosis and subsequently segregated differentially into daughter cells. During this process, at the simplest level and without factoring in other potential organelle[4,5] or cell cycle component interactions,[6,7] these membrane complexes interact with centrosomes and the cytoskeletal network to, respectively, anchor and enable correct mitotic spindle orientation for an ACD.[8-10] The distinct advantages of these invertebrate models include the ability to follow the end fate of daughter cells during successive rounds of ACD together with real-time video tracking to observe the clear segregation of established cell-fate determinants during and after the ACD process. In contrast, within the hematopoietic system, these advantages are attenuated by the absence of definitive HSC markers or cell fate determinants that could allow for investigations of successive divisions of long-term repopulating HSCs (LT-HSCs). The added factor of HSC motility outside of its niche further hinders prospective daughter cell fate analysis.

Despite these limitations, important aspects of HSC self-renewal with indirect implications for ACD as a mechanism have been reported. For example, for many decades, single-cell manipulations with more enriched HSC populations over time have documented different in vitro[11,12] and in vivo[13-15] cell fates. Further, asymmetric segregation of proteins within the hematopoietic system has also been reported previously,[16-18] but did not confirm alterations in cell fate because in vivo daughter cell assays were not tenable in these studies. Other studies have used live-cell videomicroscopy of single cells derived from a population enriched for HSCs together with clonal fate of progeny as measured by in vivo repopulation assays to provide morphological clues as to the

identity of LT-HSCs; however, this was done without confirming ACD per se in this setting.[19] Far from being a critique, these examples reflect the difficulty of directly connecting ACD to daughter cell fate within the heterogeneity of the HSC system. The present study was undertaken to provide further evidence that the process of ACD is functional in HSC fate and to serve as a foundation for ongoing future studies that may allow ACD, HSC fate, and self-renewal to be directly and mechanistically linked.

Methods

Procedures for retroviral vectors, animal husbandry, HSC isolation, quantitative RT-PCR expression studies, BM cell culture, retroviral infection and transplantation, flow cytometric assessment of donor-derived hematopoiesis, Southern blot analysis of genomic DNA, competitive repopulating units (CRU) assay of HSC-enriched cells, and cell proliferation and cell death analyses were as detailed in Deneault et al.[20] All animal procedures were performed with approval from the Animal Ethic Committees of University of Montreal and Peter MacCallum Cancer Institute. For resource information, please see http://www.bioinfo.iric.ca/self-renewal/.

Confocal microscopy

Mouse adult BM and embryonic day 14.5 (E14.5) fetal liver (FL) cells were isolated independently and lineage depleted by staining with allophycocyanin (APC)–conjugated primary Abs to Gr1, B220 and Ter119 (all from BioLegend). Respective BM and FL cells were stained with anti-APC magnetic microbeads according to manufacturer guidelines (Miltenyi Biotec), and lineage positive (Lin$^+$) cells were depleted using the AUTO-MACS magnetic cell separator system (BD Biosciences). For the adult BM cells, lineage negative (Lin$^-$) cells were stained with PE-CD150, APC-CD48, PE-Cy5-Sca, and PE-Cy7-Kit conjugated Abs, and the enriched CD150$^+$48$^-$ Lin$^-$Sca$^+$Kit$^+$ (LSK) subpopulation of cells collected by flow cytometry using the FACSAria II (BD Biosciences). For the FL cells, Lin$^-$ cells were stained with PE-CD150, APC-CD48, PE-Cy5-Sca, and FITC-Mac–conjugated Abs and the enriched CD150$^+$48$^-$Sca$^+$Mac1$^+$Lin$^-$ subpopulation of cells was collected. These respective subpopulations of cells were resuspended in DMEM with 15% FBS. Respective BM- and FL-enriched subpopulations up to 50 000 cells per slide were seeded onto poly-L-lysine–coated coverslips and incubated at 37°C for 60 minutes. Cells were then fixed with 4% paraformaldehyde for 15 minutes at 4°C and permeabilized with PBS, 1% BSA, 0.1% Tween and stained with primary Abs to Ap2a2 (AP6, ab2730; Abcam) and/or Numb (ab4147; Abcam) and revealed by Alexa Fluor 488– and/or Alexa Fluor 594–labeled secondary Abs (Molecular Probes). Fluorescent images were obtained with a confocal microscope (LSM510; Zeiss).

Videomicroscopy

Freshly sorted PE-CD150$^+$/APC-CD48$^-$/PE-Cy5-Sca$^+$/PE-Cy7-cKit$^+$/Lin$^-$ BM cells from histone H2B-GFP mice were transduced with retroviral producers infected with MSCV-cherry-Ap2a2 and/or pCXIBSR-venus-Numb vectors for 3 days. Cells were then sorted based on forward and side scatter to differentiate between hematopoietic and feeder cells. Isolated hematopoietic cells in BM medium[20] were seeded into 8-mm sterile cloning discs (F378470100; Bel-Art Scienceware) placed on glass-bottom MakTek dishes (number 1.5; MatTek) of a confluent and irradiated (1500 cGy of ^{137}Cs γ radiation) layer of either NIH 3T3 or OP9 cells. Video imaging comprised 3 colors (green fluorescence, red fluorescence, and transmitted light) and 4 z-sections 2.5 μm apart every 15 minutes for 24 hours with an Olympus 60×/1.42 numerical aperture oil-immersion lens and a Photometric CoolSnap HQ2 camera on a DeltaVision video microscope fitted with a 37°C environmental chamber (Applied Precision). Video analyses were performed with softWoRxExplorer Version 2.0 (Applied Precision) and Imaris software (Bitplane Scientific Software).

Statistical analysis

Statistical significance was determined with the 2-tailed Student t test.

Results

Candidate polarity screen for HSC expansion

Using existing expression databases[21] and literature analyses, we compiled a candidate gene list of polarity cell-fate determinants for initial gene-expression profiling. Given the heterogeneity of the HSC compartment, we used 2 established enriched HSC subpopulations, the CD150$^+$48$^-$41$^-$Lin$^-$ and the CD49b$^-$rhodamine^{low} LSK cells, for assessment (Figure 1A-C and supplemental Table 1, available on the *Blood* Web site; see the Supplemental Materials link at the top of the online article). These gene-expression profiles show that a broad range of polarity candidates are highly and differentially expressed in both HSCs and leukemia cells (Figure 1A-C). To assess whether polarity genes would be altered by an established HSC expansion factor,[22] we profiled gene-expression levels of a subset of candidate genes after HSCs were transduced with *HoxB4* and with MSCV vector (Figure 1D). These data show that *HoxB4* does not affect this subset of polarity candidate genes at the mRNA level.

Based on our gene-expression profiles (Figure 1), 43 (∼ 60%) of the candidates were chosen to assess whether any of these genes could alter the fate of LT-HSCs using an established gain-of-function in vitro to in vivo assay (for full details, see Deneault et al[20]; Figure 2A-B and http://www.bioinfo.iric.ca/self-renewal/). The theoretical essence of this screen is based on the relative inability of HSCs to preserve functional identity (ie, self-renewal) during a period of in vitro culture when apoptosis or differentiation are the predominant HSC fate, and as measured by the relative absence of in vivo repopulation of sublethally irradiated recipients after transplantation. In contrast, transduction by a candidate fate-transforming gene to either maintain or expand the HSC population after in vitro culture would result in a predominant donor-derived in vivo transplantation output. Briefly, 1500 enriched CD150$^+$48$^-$Lin$^-$ HSCs (equivalent to ∼ 62 CRUs per well or 8 CRUs per transplanted mouse[20]) from CD45.1 mice were transduced with high titer retroviruses produced from transfections with the candidate genes and cultured in vitro for 7 days before transplantation into 3 recipient CD45.2 mice. Every 4 weeks up to 16 weeks, donor-derived WBC reconstitution was assessed. The 2 negative controls were HSCs transduced with vectors pKOF and MSCV, and the 2 positive controls were transduced with the NUP98-HOXA10 fusion (*NA10HD*)[23] and *HoxB4*,[22,24] with the positive cutoff set at the latter's mean reconstitution of 30% at 16 weeks. This primary screen revealed 6 (14%) positive candidates that significantly increased hematopoietic reconstitution: *Ap2a2*, *Gpsm2*, *Tmod1*, *Kif3a*, *Racgap1*, and *Ccnb1*. See Figure 2B and supplemental Table 2 for full results without (day 0) and with (day 7) in vitro culture. We initially focused on the candidate *Ap2a2* because it was the most potent HSC expansion gene within the screening experiments (Figure 2B). The other positive candidates will be analyzed subsequently.

Validation and self-renewal of *Ap2a2*-transduced HSCs in vitro

To validate *Ap2a2* as a genuine candidate, we performed 3 further independent in vitro to in vivo assays with the mean reconstitution levels from each assay supporting the initial screen results (Figure
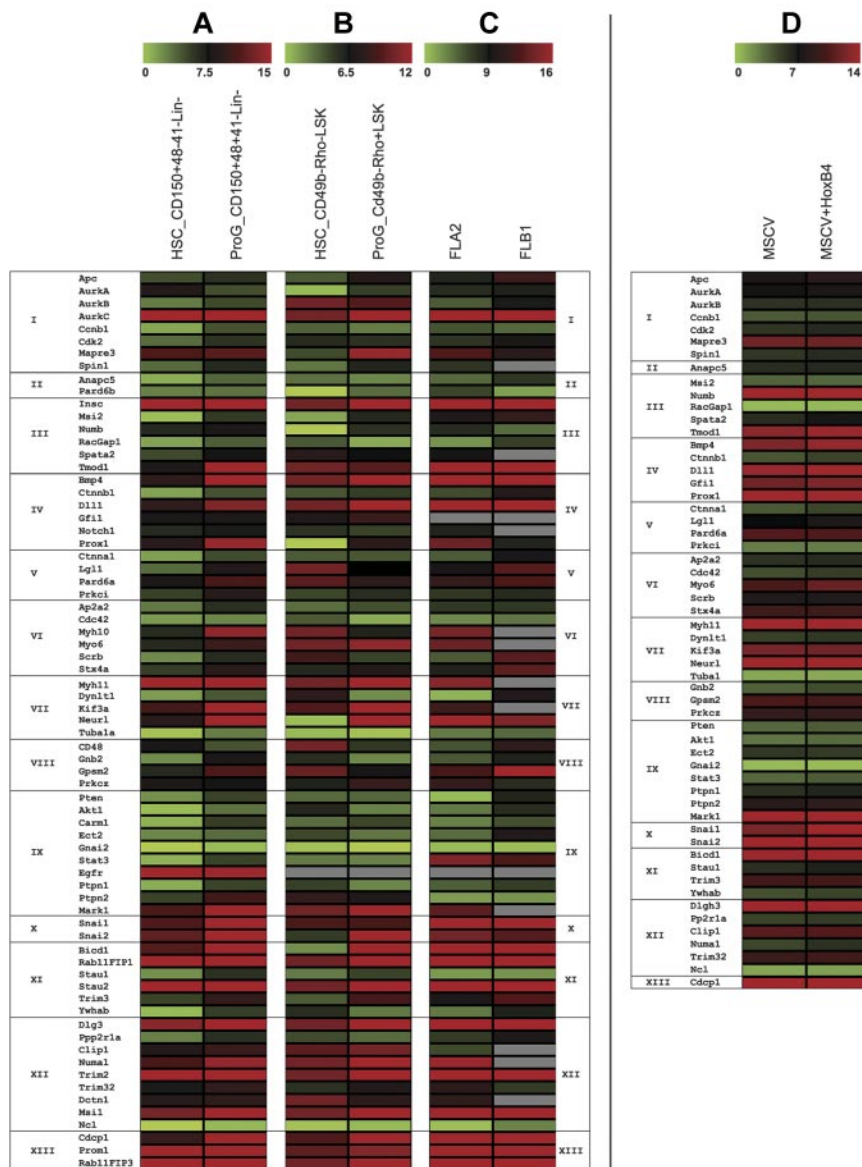
Figure 1. Gene-expression profiles of HSC polarity fate determinants. Candidate genes were classified according to Gene Ontology (GO) groups (see below) based initially on biologic process (Groups I-XI). In the absence of a biologic process, they were then based on molecular function (Group XII) and cellular component (Group XIII). The expression of these candidate genes was performed on purified HSC populations compared with more differentiated progenitors. Each dataset is represented by the mean average δCt from 2 experiments in which for each respective reference range, the lowest numbers (green bars) correspond to the highest transcript copy numbers. Shown are gene expressions from (A) HSCs sorted on CD150+48−41−Lin− (with a stem cell frequency of 1 in 10 based on CRUs; data not shown) and progenitors CD150+48+41−Lin− (B) HSCs sorted on CD49b−rhodamine^low LSK (with a stem cell frequency of 1 in 8 based on CRUs, data not shown) and progenitors CD49b−rhodamine^high LSKs, and (C) 2 independent murine leukemias, FLA2 and FLB1, derived from HoxA9+Meis1 transduced FL cells, that differ in leukemia stem cell frequency of, respectively, 1 in 1.4 and 1 in 347 (based on previous CRU, data not shown). (D) A subset of these candidate genes were profiled after CD150+48−41−Lin− HSCs were transduced with the established expansion factor *HoxB4* and compared with MSCV vector alone transduced HSCs. GO Groups: I_GO_7049 cell cycle; II_51301 cell division; III_30154 cell differentiation; IV_45165 cell-fate commitment; V_7163 establishment or maintenance of cell polarity; VI_16192 vesicle mediated transport; VII_16459 myosin complex; _7017 microtubule-based process; VIII_7154 cell communication; IX_50678, _7242, _7169, _6468 receptor signaling pathways; X_48729 tissue morphogenesis; and, _43066 negative regulation of apoptosis; XI_33036, _51234 macromolecule and establishment of localization; XII_5515, _8092 protein and cytoskeleton binding; _3774 motor activity; _8266, _3723 RNA binding; and XIII_5886,16 020 membrane; _45177 apical part of cell. From studies shown in panels A through C, a scoring criteria (data not shown) based on the absolute average δCt and the relative expression in the stem versus progenitor cell populations was used to quantify the candidates chosen for the in vitro to in vivo overexpression screen (see also supplemental Table 1).

2C and *Ap2a2* gene results at http://www.bioinfo.iric.ca/self-renewal/). We also confirmed the expression of the Ap2a2 protein from NIH 3T3 (ie, GP+E-86) producer cells used during HSC transduction (Figure 2D). To ensure that aberrant retroviral insertion was not aiding the reconstitution advantage of *Ap2a2*-transduced HSCs, we performed clonal analysis of cells obtained from BM and thymus from 2 reconstituted mice (Figure 2E). This showed the presence of many clones in different mice, together with multipotentiality of transduced cells, because the same clones were present in both myeloid (BM) and lymphoid (thymus) predominated tissues of the same mouse. Further evidence of the multipotency was provided by flow cytometric analysis from a representative recipient mouse transplanted with *Ap2a2*-transduced HSCs sorted on donor CD45.1 cells with B-cell (B220), monocyte-macrophage (CD11b), and mature T-cell (CD4 and CD8) reconstitution (Figure 2F).

CRU assays were performed to validate and determine whether *Ap2a2*-transduced HSCs expand and/or are maintained ex vivo[24,25] (Figure 3A). Initially, (based on day 0 CRU assays) 200 CD150+48−Lin− HSCs from CD45.1 mice were transduced with *Ap2a2* pKOF vector (for the negative control) and *HoxB4* and

NA10HD (for the positive controls), cultured for 7 days in vitro, and transplanted in limiting cell numbers into sublethally irradiated CD45.2 recipients. Analyses of donor WBC reconstitution at 12 weeks were used to determine CRU frequencies. The respective frequencies were: pKOF (1 in 457 107), *Ap2a2* (1 in 136 135), *HoxB4* (1 in 8165), and *NA10HD* (1 in 1036) cells (Figure 3A). Interestingly, when these calculated CRU frequencies were analyzed in relation to the input 200 CRU cells at day 0 and the absolute numbers of cells at the end of the in vitro culture period, the following differences were found: a 29-fold reduction in CRU cells after transduction with pKOF, an 11-fold reduction in *Ap2a2*, a 2-fold increase in *HoxB4*, and a 19-fold increase in *NA10HD*. These results suggest that the enhanced HSC activity invoked by Ap2a2 transduction may be attributable to a relative reduced loss and/or maintenance of HSC numbers in vitro coupled with a proliferative effect in vivo after transplantation.

To look further for self-renewal of expansion in vitro, we looked for clonal expansion of *Ap2a2*-transduced HSCs by analyses of proviral integration patterns from 11 primary recipients (Figure 3B). Based on the absence of the same clones in any of these 11 mice from 4 independent cell culture populations (Figure 3B),

Figure 2. Polarity screen to identify agonists of HSC expansion. (A) Schematic representation of the screening approach. (B) Summary of the HSC polarity genes in vitro to in vivo gain of function screen. Respective gene plasmids are labeled (∧ or *) in relation to respective vector backbones (see also supplemental Table 2). (C) Mean ± SEM of 3 validation experiments. (D) Protein expression of AP2A2 in transfected GP+E-86 cells. (E) Southern blot analysis on DNA extracted from BM (BM) and thymic tissues of 2 mice (mice 1 and 2), and hybridized with a green fluorescent protein–specific probe. (F) Flow cytometry from an *Ap2a2*-transduced recipient mouse sorted on donor CD45.1 cells.
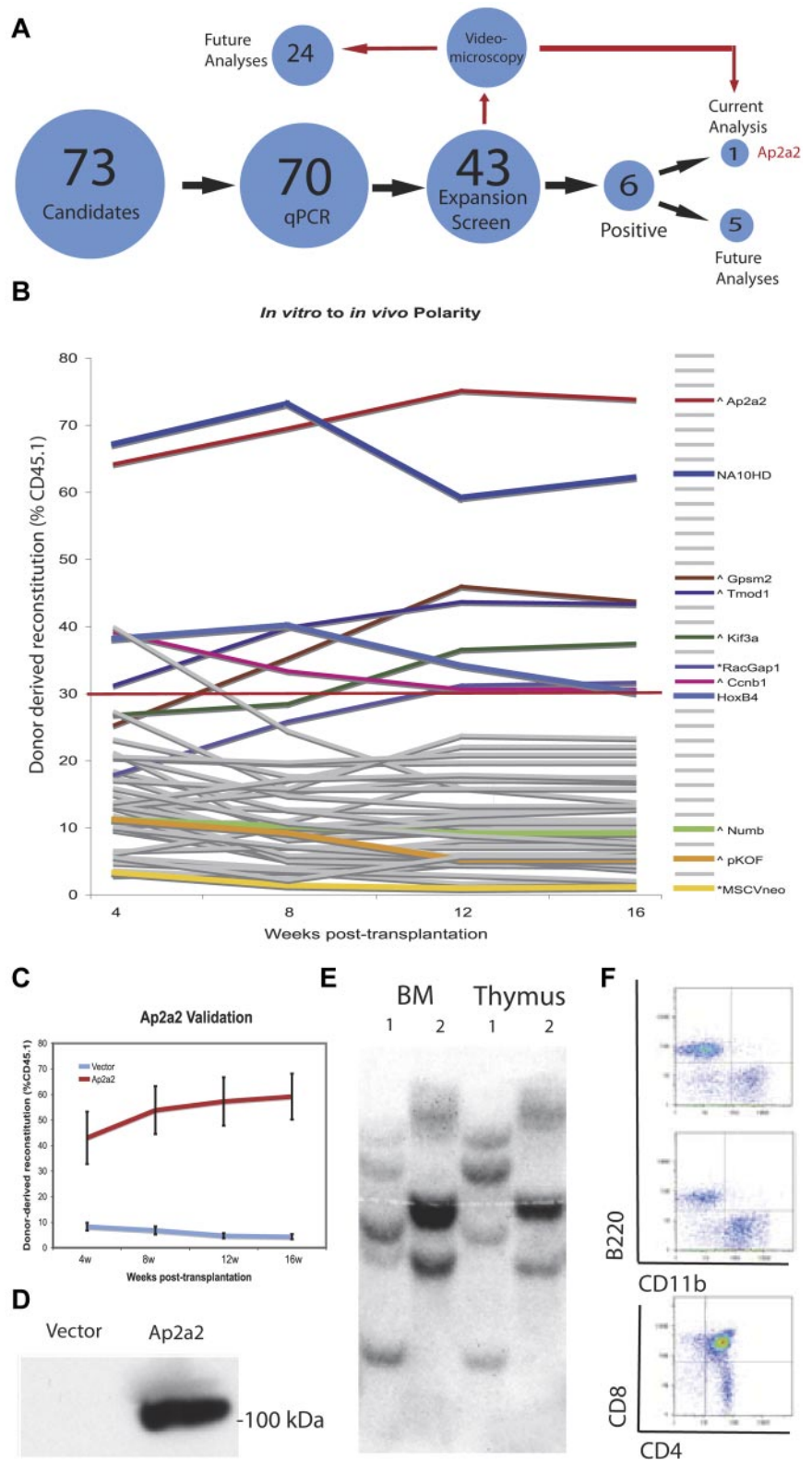
we surmised that there was no clear evidence of predominant in vitro symmetric self-renewal with *Ap2a2* during our 7 days of culture. In contrast, similar clonal analyses from the majority of transcriptional positive regulators of HSCs from our previous screen[20] showed symmetric self-renewal divisions in vitro.

In the context of seemingly limited numbers of *Ap2a2*-transduced HSCs providing enhanced HSC function, we quantified phenotypic LT-HSC populations and the proliferative output of *Ap2a2*-transduced HSCs. From a separate cohort of CD45.1 donor mice, CD150$^+$48$^-$Lin$^-$ HSCs were transduced with vector and *Ap2a2* and in vitro cultured before transplantation with 200 000 CD45.2 BM competitor cells into sublethally irradiated CD45.2 recipients. We measured the percentage of LT-HSCs (CD150$^+$48$^-$LSK) within the donor CD45.1-transduced and
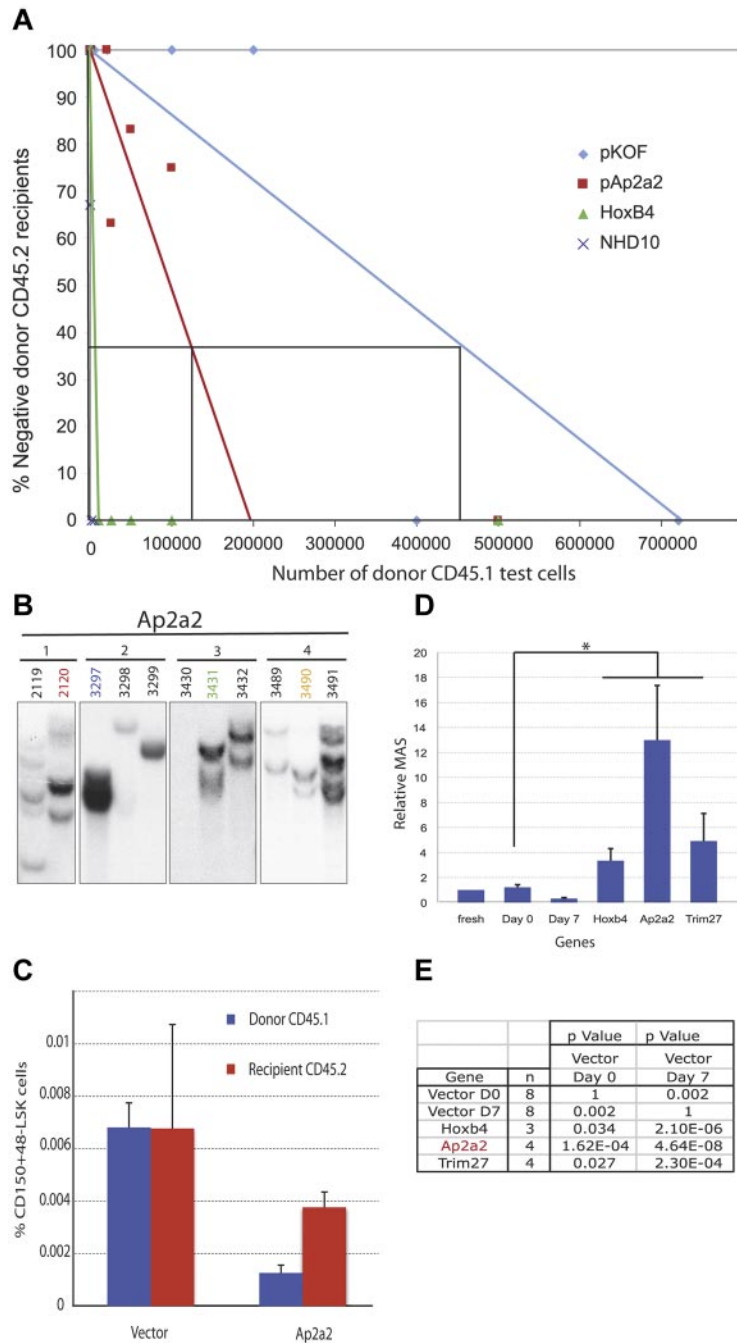
Figure 3. Analyses of *Ap2a2*-transduced HSCs in vitro. Cells used for panels A through E are CD150⁺48⁻Lin⁻. (A) CRU assay in primary recipients with respective transduced cells. (B) Southern blots with GFP-specific probe on BM of 11 recipient mice (2119-3491) from 4 independent culture wells of *Ap2a2*-transduced HSCs (1-4). (C) Donor-derived compared with competitor, recipient-derived CD150⁺48⁻LSK LT-HSCs in BM from primary recipients analyzed at 20 weeks after transplantation with vector- and *Ap2a2*-transduced HSCs. (D) MAS for transplanted *Ap2a2*-transduced HSCs as calculated from data in Figure 2B and C. Because these *Ap2a2*-transduced assays were performed in conjunction with our previous overexpression screen,[20] in which the control CRU was known for freshly purified CD150⁺48⁻Lin⁻ HSCs, the published data for fresh cells, days 0 and 7 grafts, and positive grafts for *Hoxb4*- and *Trim27*-transduced cells are used as valid negative controls and positive comparators, respectively. The MAS for *Ap2a2* (*) is statistically significantly higher (see value in panel E), compared with day 0 and 7 controls. (E) *P* value for Ap2a2-transduced HSCs derived from MAS data in panel D compared with published control vectors (day 0 or 7) and the most potent HSC activators from our initial screen.[20]

		p Value	p Value
		Vector	Vector
Gene	n	Day 0	Day 7
Vector D0	8	1	0.002
Vector D7	8	0.002	1
Hoxb4	3	0.034	2.10E-06
Ap2a2	4	1.62E-04	4.64E-08
Trim27	4	0.027	2.30E-04

CD45.2 subpopulations of recipient mice 20 weeks after transplantation (Figure 3C). In the *Ap2a2*-transduced mice, the percentage of LT-HSCs was less in the donor CD45.1 population compared with the CD45.2 recipient-competitor cells (Figure 3C). In contrast, measurement of the proliferative output per *Ap2a2*-transduced LT-HSCs using the mean activity of stem cell (MAS), as detailed in our previous functional screen for HSC activity,[20] revealed a 13-fold higher MAS for *Ap2a2*-transduced LT-HSCs when normalized to freshly sorted HSCs (Figure 3D). This relative MAS activity is not only higher, but is also statistically more significant, than both *Hoxb4*-transduced and the most potent gene from our initial screen, *Trim27*-transduced cells[20] (Figure 3D-E). This suggests that *Ap2a2*-transduced HSCs possess the ability for superior proliferative output per HSC.

These studies of in vitro cultured *Ap2a2*-transduced HSCs revealed increased HSC activity in vivo (Figure 3D-E), but the absence of obvious in vitro HSC expansion based on CRU assay (Figure 3A) and clonal analyses in primary recipients (Figure 3B) or quantitative increases in LT-HSCs (Figure 3C) suggests that *Ap2a2* induces maintenance of HSCs in vitro that is translated to an in vivo proliferative advantage by either a preference for asymmetric self-renewal divisions and/or a qualitative change in LT-HSCs.

Self-renewal of Ap2a2-transduced HSCs in vivo

Secondary transplantation assays were performed to assess whether *Ap2a2*-transduced LT-HSCs retained self-renewal capacity in vivo. Eleven primary *Ap2a2*-transduced mice (Figure 3B mice 2119-3491) and another 5 mice (Figure 4A mice 5317-5343) from

Figure 4. Self-renewal of Ap2a2-transduced HSCs in vivo. (A) Analyses of secondary transplantation recipients. Donor CD45.1 reconstitution in numbered primary donor (pd) mice and transplanted secondary recipient (sr) mice. Horizontal bar shows the mean level of reconstitution for each (sr) group. (B) In vivo clonal analyses of self-renewal. Southern blots with GFP-specific probe on BM from 1 (pd) mouse from each *Ap2a2*-transduced well (1-4 in Figure 3B) and their respective (sr) mice (as numbered and indicated by respective color codes). (C) CRU assay in secondary recipients. From 3 further independent in vitro to in vivo assays with vector-transduced and *Ap2a2*-transduced CD45.2 donor CD150$^+$48$^-$Lin$^-$ HSCs transplanted into CD45.1 recipients: 1 representative primary CD45.1 recipient mouse from each assay was taken at 20 weeks after transplantation (supplemental Figure 1A). From these 3 vector-transduced and 3 *Ap2a2*-transduced primary recipient mice, BM cells were flow sorted for donor CD45.2 cells. Equivalent limiting donor cell numbers, together with 200 000 CD45.1 competitor BM cells, were transplanted into sublethally irradiated secondary CD45.1 recipients for assessment of donor reconstitution. Analyses were done 16 weeks after secondary transplantation via WEHI bioinformatics ELDA software (http://bioinf.wehi.edu.au/software/elda/). (D) Quantification of CD45.2 donor reconstitution in secondary recipients with respective transduced-HSCs from CRUs in panel C. Significance for recipients transplanted with, respectively, 100 000, 200 000, and 500 000 *Ap2a2*- compared with vector-transduced cells are $P = .02$, $P = .03$, and $P = .01$ (*). (E) Donor-derived compared with recipient-derived LSK cells in BM from secondary recipients analyzed at 20 weeks after transplantation. Given the minimal CD45.2 donor repopulation in vector-transduced recipient mice (D), the 2 vector-transduced mice together with the competitor CD45.1 subpopulations from the *Ap2a2*-transduced recipients were assessed together as the competitor CD45.1 population and compared with the *Ap2a2*-transduced CD45.2 donor populations for respective LSK%. *$P = .02$.
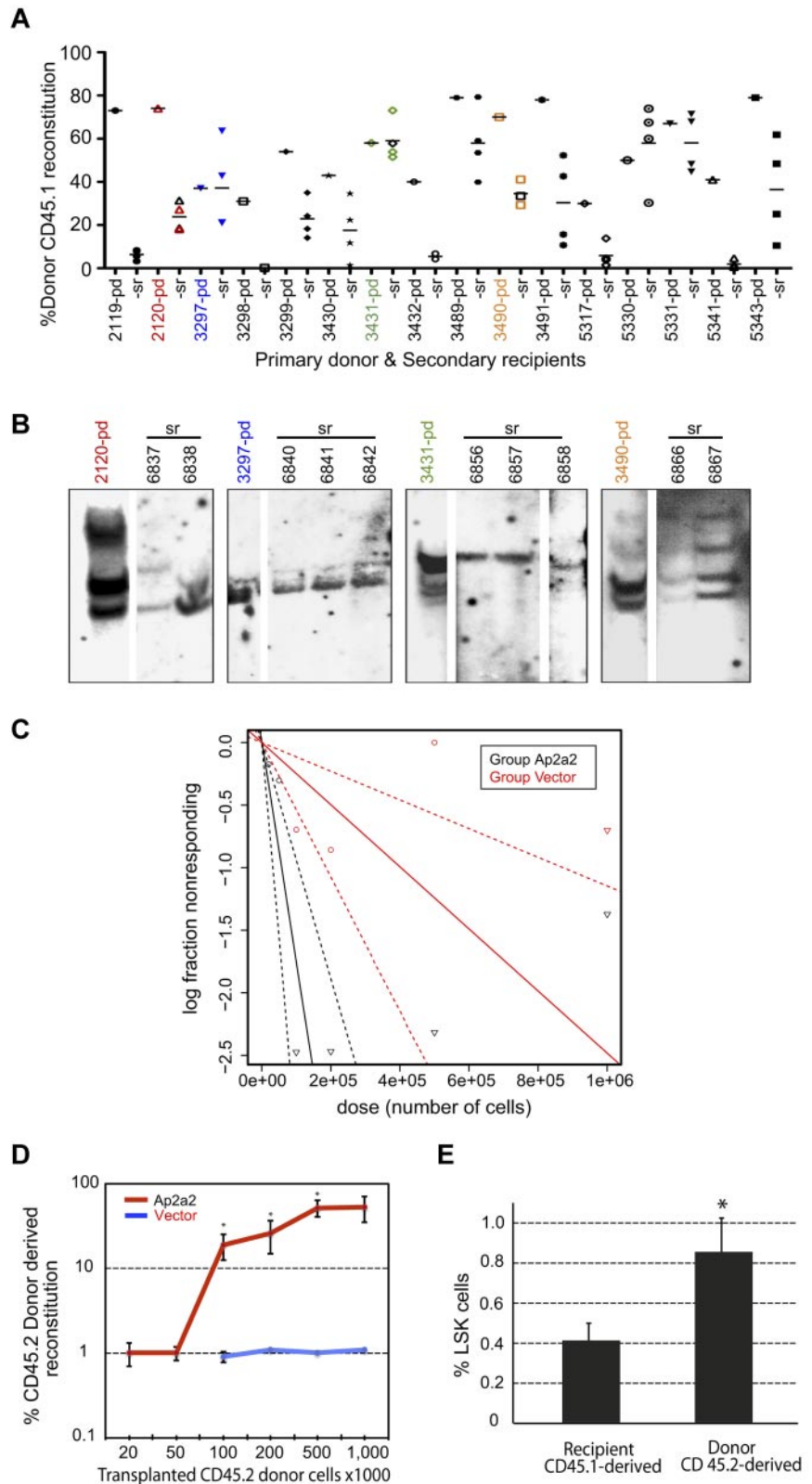
another experiment with high *Ap2a2*-transduced HSC donor reconstitution were killed at ≥ 16 weeks and used as primary donors. Approximately 5×10^6 cells (without congenic helper cells) were transplanted into 4 secondary recipients per primary mouse (Figure 4A-B) and analyzed 23 weeks after transplantation. Positive donor reconstitution in the majority of secondary recipients confirmed

that *Ap2a2*-transduced HSCs exhibited prolonged in vivo activity within the primary mouse (Figure 4A). Secondary recipient BM and thymic tissue gated on donor CD45.1 expressed markers for B-cell, myeloid cell, and T-cell lineages, suggesting that donor cells retained lymphomyeloid differentiation capacity (data not shown). To assess for in vivo clonal composition, one primary donor from

each independent well of the *Ap2a2*-transduced cell population shown in Figure 3B, together with respective multiple secondary recipients, were analyzed for proviral integrations (Figure 4A-B). This showed at least 2 independent clones from each primary donor in multiple respective secondary recipients (Figure 4B), which is consistent with clonal in vivo symmetric cell divisions.

Because clonal symmetrical HSC divisions may be expected to occur in the transplantation setting, to quantify the in vivo self-renewal of *Ap2a2*-transduced HSCs, we performed CRU assays in another batch of secondary recipients (Figure 4C-E). At 16 weeks after transplantation, the CRU frequency for the vector-transduced cohort was 1 in 402 807 cells compared with 1 in 57 428 cells for the *Ap2a2*-transduced cohort of secondary recipient mice (Figure 4C and supplemental Figure 1A-C). Furthermore, for equivalent transplanted donor cell doses, *Ap2a2*-transduced HSCs provided significantly greater and incremental dose-dependent reconstitution compared with vector-transduced HSCs (Figure 4D).

To correlate and quantify HSC numbers after in vivo self-renewal, 10 of these secondary recipient mice (2 vector transduced and 8 *Ap2a2* transduced) were killed at 20 weeks for analyses of donor CD45.2-derived versus competitor CD45.1-derived BM LSK subpopulations (Figure 4E). When normalized to an equivalent 200 000 CD45.1 competitor cell dose, the percentage of LSK cells in the *Ap2a2*-transduced CD45.2-derived population showed a modest but statistically significant 2-fold greater increase in the *Ap2a2*-transduced CD45.2 donor-derived LSK population (Figure 4E).

These secondary recipients reconstitution results show that *Ap2a2*-transduced HSCs have a modest quantitative in vivo self-renewal expansion yet maintain potent HSC reconstitution activity (Figure 4C-E). These results are similar to the in vitro to in vivo transplantation assay results in primary recipients (Figure 3A-E), in which the increased *Ap2a2*-transduced HSC reconstitution is also seen without a significant corresponding quantitative increase in HSCs. This suggests that the *Ap2a2*-induced enhanced HSC activity occurs mostly in vivo both in primary and secondary recipients.

Effect of *Ap2a2* shRNA in HSCs

We further investigated the role of *Ap2a2* in HSC activity by studying the impact of shRNAs that reduce *Ap2a2* mRNA levels by 50%-90% within the context of our in vitro to in vivo reconstitution assay (supplemental Figure 2A-B). Results from these experiments suggest that *Ap2a2* is dispensable for hematopoiesis. Homing efficiency as measured by the percentage of donor CD45.2-transduced cells in the BM of recipients 24 hours after transplantation and annexin V apoptosis assays of respective transduced HSCs cultured for 7 days in vitro revealed no significant differences between 3-, 4-, and 5-shAp2a2–transduced HSCs compared with shRNA luciferase–transduced CD150+48−Lin− HSCs (data not shown).

These Ap2a2 knockdown assay results, together with the findings from our previous screen of non-cell-autonomous activity for other positive regulators of HSC expansion during in vitro culture,[20] led us to assess whether such activity was also aiding the in vivo effect of *Ap2a2*-transduced cells. Using non-viral-producing NIH 3T3 cells for transfection with *Ap2a2*, followed by subsequent HSC coculture and transplantation (for details, see Deneault et al[20]), we found no evidence for non-cell-autonomous contribution (data not shown). We conclude that overexpression of Ap2a2-transduced HSCs results in enhanced HSC activity after in vivo transplantation, whereas knockdown of Ap2a2 in HSCs

suggests that Ap2a2 has a redundant role within the limits of the in vitro culture and transplantation assay.

Evaluation of *Ap2a2*-transduced HSCs

We next assessed whether we could detect qualitative differences in Ap2a2-transduced HSCs by looking at the effects of *Ap2a2* overexpression on proliferation, survival, or differentiation of CD150+48−Lin− cells. The absolute cell count after in vitro culture of CD150+48−Lin− cells transduced with pKOF, *Ap2a2*, *HoxB4*, and *NA10HD* (60%-69% gene transfer) showed that the number of *Ap2a2*-transduced cells was not enhanced (Figure 5A). In vitro proliferation analyses with methylcellulose colony forming assays showed that *Ap2a2*-transduced HSC progenitor cells were capable of producing the full spectrum of differentiated colonies (Figure 5B) with no differences in colony size (data not shown). Differentiation arrest has been found to contribute to the prominent HSC expansion mediated by *HoxB4* and *NA10HD*.[25] However, *Ap2a2*-transduced HSCs show a limited differentiation arrest compared with *NA10HD*-transduced HSCs (Figure 5C-D blue bars).

Other key cellular pathways assessed via in vitro analyses of LSK cells transduced with and without *Ap2a2* for 5 days were: cell cycle by Hoechst/phospho-histone H3 and bromodeoxyuridine pulse and chase for 24 hours, cell death by annexin V/propidium iodide, senescence by β-galactosidase, and measurement of cell divisions using cell track violet for up to 10 days in culture. None of these assays showed differences between *Ap2a2*-transduced and vector-transduced cells (data not shown). Ap2a2 modestly inhibits primitive hematopoietic cell differentiation in vitro without altering apoptosis and the other key cellular processes involved in self-renewal.

Another important property of the stem cell is the ability to remain quiescent until actively required. This concept has been highlighted within the hematopoietic system by the identification of a small population of multipotent, dormant LT-HSCs.[26,27] To assess this in vivo, we assessed the cell-cycle status from 10 secondary recipients killed at 20 weeks. The LSK subpopulations from the *Ap2a2*-transduced CD45.2 donor-derived and competitor CD45.1-derived subpopulations were stained with DAPI-Ki67 to assess in particular the percentage of cells in G_0. There was no difference in G_0 or any other cell-cycle parameters between the 2 cell subpopulations (data not shown).

Because the dormant LT-HSC population is both small and heterogenous, detection of a difference at the bulk population level would be difficult. To circumvent this and to further investigate the *Ap2a2*-quiescence link, we isolated from independent sorts batches of 30-50 cells of the LT-HSC and multipotent intermediate-term HSC (IT-HSC)[28] populations while in quiescence and in cell cycle for *Ap2a2* expression. This IT-HSC population, isolated in the CD49b^hi rhodamine^low LSK fraction and separable from the classic short-term repopulating HSCs, generates multilineage clones that expand through to 8 weeks. Although the clones subsequently regress, lymphoid components remain detectable beyond 6 months. In contrast, the established LT-HSCs (CD49b^− rhodamine^low LSK) sustain multilineage reconstitution beyond 6 months and for the lifetime of the animal. Gene expression was measured on Affymetrix microarrays (for details, see Benveniste et al[28]). These results (supplemental Figure 2C) suggest that *Ap2a2*, and to a lesser degree *Numb*, are preferentially expressed in the quiescent versus the cycling state of both the LT-HSCs and IT-HSCs. To quantify these microarray results, we performed quantitative RT-PCR on paired G_0-quiescence and cycling LT-HSC and IT-HSC populations from 7 independent mouse sorts (Figure 5E). These results confirmed the microarray findings and in particular showed
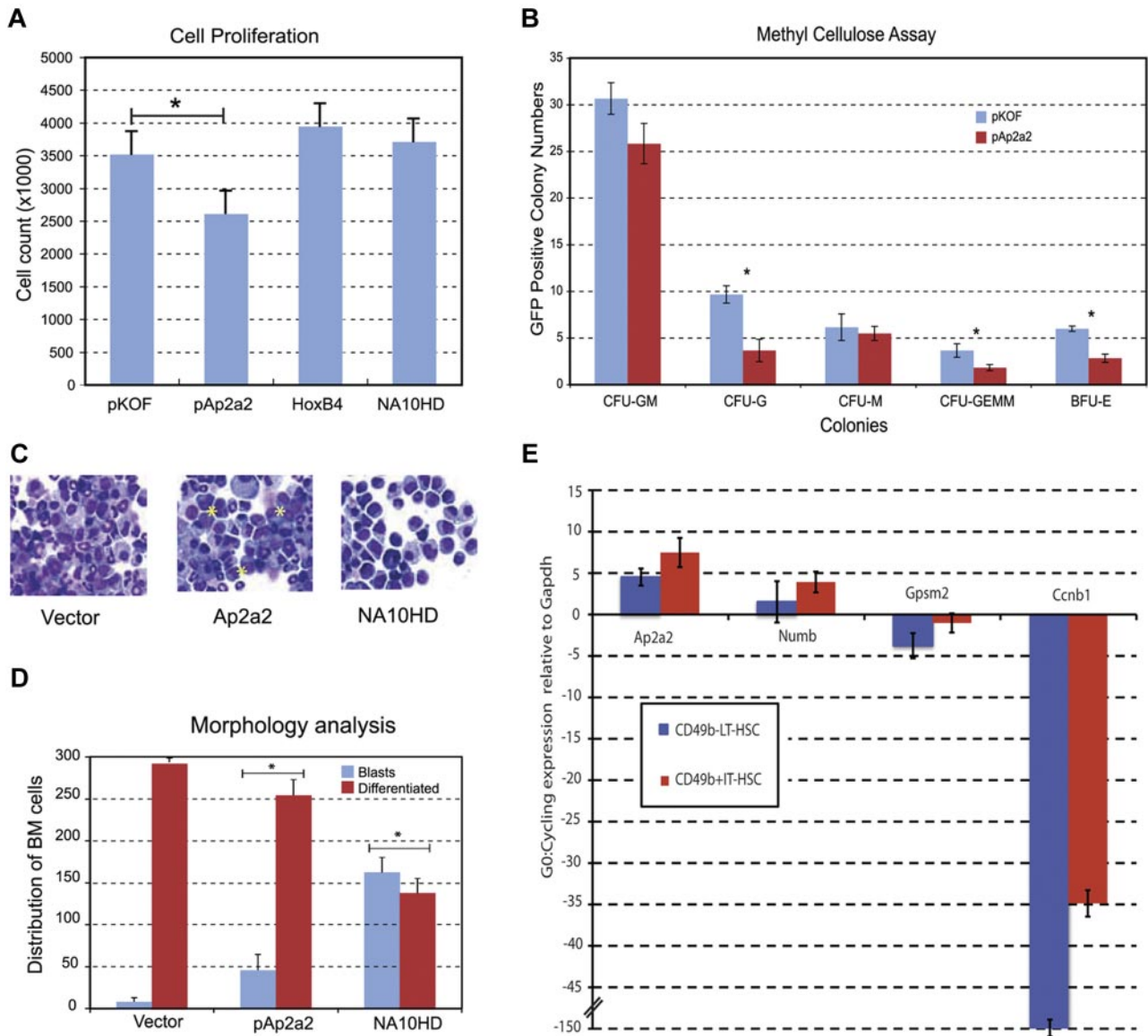
Figure 5. Qualitative effects of *Ap2a2*-transduced HSCs. (A) Cell proliferation counts of respective green fluorescent protein–positive (GFP$^+$) transduced cells. *P = .03. Values presented are means ± SEM from independent experiments for pKOF (n = 3), pAp2a2 (n = 4), HoxB4 (n = 4), and NA10HD (n = 2). (B) Methylcellulose assays for in vitro proliferation and differentiation. Values presented are means ± SEM number of GFP positive colonies from 3 independent experiments. Statistical significance between vector and *Ap2a2* for CFU-G, *P < .001; CFU-GEMM, *P = .02; and BFU-E, *P = .002. (C) Cytospin morphology of respective GFP$^+$-transduced cells. Asterisks indicate clusters of undifferentiated blasts. (D) Means ± SEM from 300 cell differential counts with respective GFP$^+$-transduced cells from independent experiments for vector (n = 5), pAp2a2 (n = 5), and NA10HD (n = 2). Statistical significance between vector and Ap2a2 was P = .002 and for NA10HD, *P ≤ .0001). (E) Quantitative RT-PCR expressed as G$_0$:cycling ratio (mean ± SEM) from LT-HSC (CD49b$^-$Rho^{low}LSK) and IT-HSC (CD49b$^+$Rho^{low}LSK) populations paired for G$_0$-quiescent and cycling from 7 independent sorts. Both *Ccnb1* (Cyclin B1) as part of the cell-cycle network[6] and *Gpsm2*, which is involved in active mitotic spindle orientation,[8-10] serve as effective internal controls given their (expected) relative higher expression during cycling (see also supplemental Figure 2C).

that Ap2a2 mRNA expression was, respectively, 4.5- and 7.5-fold increased in the LT-HSCs and IT-HSCs during quiescence compared with the cycling state.

Disparate *Ap2a2* and Numb localization in HSC

In our screen, *Ap2a2* was chosen as a candidate based on its association with the cell-fate determinant *Numb*. AP2A2 is the large α adaptin subunit of the adaptor-protein 2 (AP-2) heterotetrameric complex that is integral to clathrin-coated pits during endocytosis of transmembrane receptors.[29,30] AP2A2 has been shown to bind NUMB in mammalian cells,[31,32] and in the *Drosophila* sensory organ precursor system, it is hypothesized that AP2A2 binding to NUMB allows the latter to be transported to the cell membrane for Notch receptor inhibition.[32] Within these

contexts, we investigated the relationship between AP2A2 and NUMB localization in purified hematopoietic cells.

Initially, we analyzed adult CD150$^+$48$^-$ LSK cells for endogenous localization of both proteins. Both AP2A2 and NUMB were localized in distinct vesicles (Figure 6A), but, surprisingly, the majority of these respective vesicles were not colocalized (Figure 6A-B blue bars). Especially for AP2A2, individual vesicles appeared to coalesce as cytoplasmic clusters (Figure 6C). These AP2A2 and NUMB clusters more frequently colocalized (Figure 6B-C red bars). Whereas AP2A2 in adult HSCs was more often localized asymmetrically in cytoplasmic clusters, in E14.5 FL CD150$^+$48$^-$Sca$^+$Mac1$^+$Lin$^-$ cells, AP2A2 and NUMB were more often distributed symmetrically at the cortical membrane (Figure 6D-E). In a smaller fraction of E14.5 FL cells, AP2A2 was
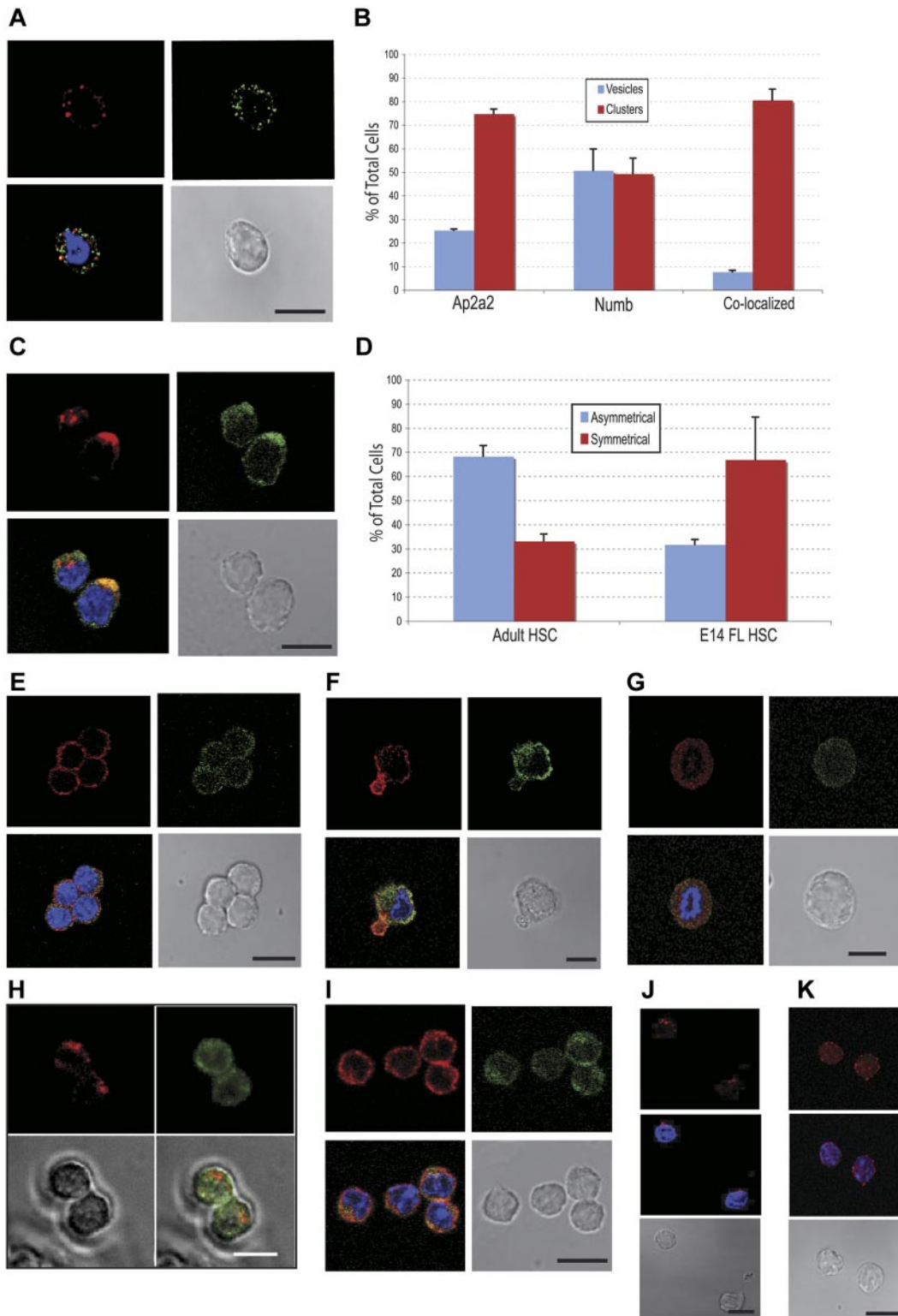
Figure 6. Endogenous AP2A2 localization in hematopoietic and leukemic cells. All subsequent cells stained for AP2A2 (Cy3-red), NUMB (FITC-green), and nucleus (DAPI-blue). (A) Adult CD150$^+$48$^-$LSK cell showing disparate AP2A2 and Numb vesicles. (B) Localization of endogenous AP2A2 and NUMB in CD 150$^+$48$^-$LSK HSCs. Definitions were as follows: vesicles, if vesicles are clear and distinct (see panel A); clusters, if any vesicles are coalesced (see panel C); colocalized, if vesicles or clusters are yellow when merged (see panels A and C). Total number of cells, N = 75. Colocalization percentage for vesicles, n = 39 cells; colocalization percentage for clusters, n = 36 cells. Values represent means ± SEM from 2 independent experiments. (C) Adult CD150$^+$48$^-$LSK cells showing asymmetric AP2A2 and NUMB clusters that are (lower cell) or not (top cell) colocalized. (D) Comparison of AP2A2 distribution in adult HSCs (n = 120 from 3 independent experiments) versus E14.5 FL HSCs (n = 127 from 2 independent experiments). Asymmetric defined arbitrarily as distinctly more AP2A2 vesicles on half of the HSCs in any plane (panels A and E are symmetric; panels C and F asymmetric). Values represent means ± SEM. (E) E14.5 FL CD150$^+$48$^-$Sca$^+$Mac1$^+$Lin$^-$ cells with symmetric distribution. (F) E14.5 CD150$^+$48$^-$Sca$^+$Mac1$^+$Lin$^-$ cell exhibiting asymmetric AP2A2 with symmetric NUMB. (G) A representative FL E14.5 CD150$^+$48$^-$Sca$^+$Mac1$^+$Lin$^-$ cell during mitosis showing endogenous AP2A2 and NUMB as diffusely symmetric vesicles that are essentially not colocalized (n = 7 cells in mitoses). (H) Still frames from live-cell videomicroscopy of representative adult CD150$^+$48$^-$LSK cell cotransduced with cherry-*Ap2a2* (Cherry-red) and venus-*Numb* (FITC-green) constructs showing the absence of colocalization during mitosis. Total of n = 20 cells seen in mitoses. From 2 independent experiments, 17 of 20 cells (85%) seen in mitoses showed absence of colocalization. (I) FLA2 leukemia cells stained for Ap2a2 and NUMB. (J) Adult CD150$^+$48$^-$LSK cells transduced with vector alone and (K) *HoxB4*, then stained for AP2A2, (see supplemental Figure 2B). All confocal images were acquired with an inverted LSM 510 microscope (Carl Zeiss) using Planapochromat 63×/1.4 numerical oil lens objective (Carl Zeiss) and analyzed with LSM Version 3.2 software (Carl Zeiss). All scale bars indicate 10 μm.

localized asymmetrically, and often when NUMB remained symmetrically distributed (Figure 6F). In both E14.5 FL CD150$^+$48$^-$Sca$^+$Mac1$^+$Lin$^-$ and adult CD150$^+$48$^-$LSK cells during mitoses, the asynchronous distribution of Ap2a2 and Numb vesicles persisted (Figure 6G-H).

Recent studies[18,33,34] have suggested that an underlying mechanism of mammalian cancer cell expansion includes disruption of the balance between symmetric cell division (SCD) and ACD. We analyzed the distribution of AP2A2 and NUMB in 2 murine myeloid leukemia lines derived in our laboratory (FLA2 and FLB1; Figure 6I). In both lines, the symmetric distribution patterns resembled that found in E14.5 FL CD150$^+$48$^-$Sca$^+$Mac1$^+$Lin$^-$ cells (compare Figure 6E with I). This may infer that leukemia cells and primitive hematopoietic cells during development are balanced toward SCD pathways that theoretically drive their expansion. Interestingly, when we transduced adult CD150$^+$48$^-$LSK cells with the expansion factors *HoxB4* or *NA10HD*, the AP2A2 distribution was altered from a predominantly asymmetric to symmetric pattern (Figure 6J-K and supplemental Figure 2D). This change in Ap2a2 protein distribution induced by *HoxB4* is in contrast to the absence of change at the mRNA level (Figure 1D), and suggests that a relocalization of fate determinant(s) may contribute to *HoxB4*- and *NA10HD*-induced HSC expansion.

Ap2a2 segregation during HSC mitosis

Another important aspect of our investigations was to identify potential cell-fate determinants that would clearly delineate an ACD, with the eventual aim of prospective isolation of daughter cells for further single progeny cell studies. Specifically for this purpose, we generated 28 candidates (Figure 2A and http://www.bioinfo.iric.ca/self-renewal/) fused in-frame with fluorescence proteins for live-cell videomicroscopy. In investigating ACD, the overexpression of a polarity factor with possible loss of polarity could theoretically skew mitoses toward SCD and thereby mask potential ACD mitoses. However, conversely and importantly, within this context, any candidate actually seen to asymmetrically segregate at division could be argued to be using stable intrinsic pathway(s) for ACD.

Based on this screen and on our complementary shRNA screen,[35] we initially video-screened *Ap2a2*, *Numb*, and *Par6α* cherry fusions. Of these candidates, only AP2A2 has shown clear asymmetric segregation at mitosis in purified HSCs, suggesting a possible specificity for *Ap2a2* in ACD. During an ACD, cytoplasmic AP2A2 vesicles cluster asymmetrically during interphase and throughout mitosis before preferential segregation into only one daughter cell at division (Figure 7A-B and supplemental Videos 1-3). The daughter cell with absent AP2A2 at division reexpresses AP2A2 at a variable time thereafter (Figure 7B asterisk at time 4:42:52). In contrast, during hematopoietic SCD, AP2A2 vesicles are diffusely and equally distributed throughout the cytoplasm during interphase and mitosis (Figure 7C-D and supplemental Videos 4-5).

These distinct and replicable differences in AP2A2 localization during mitoses allowed us to quantify hematopoietic cell division as either an ACD or SCD (Figure 7E blue bars), together with the percentage of successful mitoses (Figure 7E red bars). This quantification suggests that *Ap2a2*-transduced HSCs under in vitro culture conditions during the initial cell divisions enter equally into either SCD (52%) or ACD (48%; Figure 7E blue bars D3-5), but only a small percentage of those entering ACD (7%) have a successful mitotic division (Figure 7E red bar D3-5 asymmetric). Analyses at days 7-12 during the 1 week of in vitro culture showed that the majority of visualized HSCs entering mitoses have a

symmetric Ap2a2 distribution (Figure 7E blue bars of D7-12, 86% vs 14%). However, the success rate of the Ap2a2-symmetric mitoses is comparatively reduced (Figure 7E compare red bars D3-5 [45%] with D7-12 [22%] symmetric). In contrast, even though the number of cells entering ACD at days 7-12 are reduced, the percentage of successful mitotic divisions seen in those that enter ACD is increased or at least relatively maintained compared with initial analyses at days 3-5 (Figure 7E compare red bars D3-5 [7%] and D7-12 [27%] asymmetric). Although there are many variables to consider, these live-cell videomicroscopy results suggest that during the 1 week of in vitro culture, even though the overall rate of successful hematopoietic cell mitotic divisions was not high, that ACD was relatively maintained compared with SCD.

It has also been reported recently that external niche factors are able to influence the balance between ACD and SCD in hematopoietic precursors.[18] With respect to the localization of AP2A2, we have confirmed this phenomenon. In contrast to when HSCs were cultured with a NIH 3T3 layer (ie, GP+E-86 cells) as per Figure 7E (D3-5 blue bars), when cultured with OP9 feeder cells with a more HSC-supportive environment[36] (Figure 7F), the distribution of initial Ap2a2-tracked HSC divisions (D3-5) favored SCD in a ratio almost identical to that seen during coculture with the NIH 3T3 layer (compare Figure 7E D7-12 blue bars with Figure 7F blue bars). A possible interpretation of these results is that external (ie, niche-related) factors can skew the balance of ACD and SCD toward more symmetric divisions. In addition, the OP9 layer, presumably via extrinsic cues to the HSCs, increased the relative percentage of symmetric mitotic cells that successfully divided (as opposed to apoptosis; compare Figure 7E red bars of D7-12 and Figure 7F symmetric). However, the relative number of successful asymmetric mitoses seen with OP9 culture again remained relatively stable (compare Figure 7E red bars and 7F asymmetric). Whether this means that successful ACD is programmed intrinsically into primitive hematopoietic cells is another potential interpretation awaiting investigation.

Discussion

Clear supporting evidence for the presumption of ACD governing self-renewal in the hematopoietic system has been lacking. In addressing this question in the present study, we have acquired materials that have—and will continue to be—an important resource for our future studies in this field. In an established gain-of-function screen, we have identified the endocytic gene *Ap2a2* as a novel in vivo agonist of mouse LT-HSC activity. When overexpressed in populations enriched for LT-HSCs, AP2A2 clearly segregates asymmetrically during mitosis in a significant proportion of these cells. Within these contexts, we conclude that ACD is operational in primitive hematopoietic cells enriched for LT-HSCs.

The finding of *Ap2a2*-transduced HSCs maintaining enhanced HSC activity after both in vitro cultured and secondary in vivo transplantation in the relative absence of increased HSC numbers suggests that these transduced HSCs are either favored or maintained for ACD as opposed to SCD. One possibility, given the heterogeneity within even the small population of LT-HSCs, may be that the subset of dormant LT-HSCs is intrinsically restricted to ACD, thereby ensuring that one daughter HSC retains the dormant state whereas the nondormant daughter HSC undergoes expansion SCDs. Therefore, whereas Ap2a2-transduced LT-HSCs are maintained in quiescence in vitro, on in vivo transplantation, these Ap2a2-transduced dormant HSCs have a potent proliferative output. This phenomenon of clonal variability in proliferative and
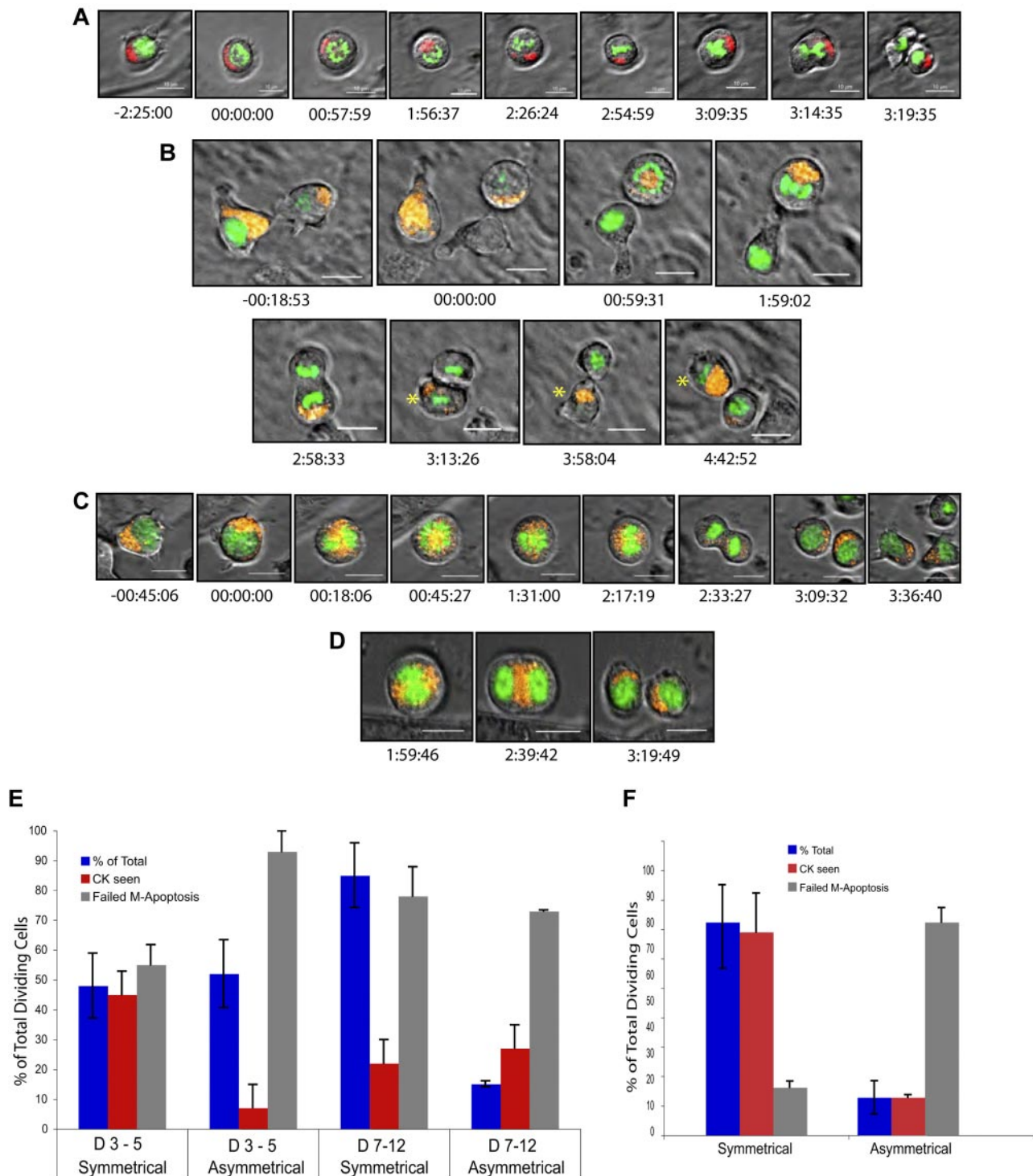
Figure 7. Asymmetric and symmetric AP2A2 during mitosis. Still frames from live-cell videomicroscopy. All cells, adult CD150+48−LSK: DNA (Fitc-green); AP2A2 (Cherry-red/orange). All time points referenced to onset of mitosis (time, 00:00:00 as hours:minutes:seconds). The mean total mitosis times for an ACD was 3:04:17 (n = 6 visualized mitotic cells) and for SCD was 2:56:04 (n = 32 visualized mitotic cells). Differences were not statistically significant. (A) Hematopoietic cell showing AP2A2 asymmetric clustering during and after cell division into daughter cells. (B) Hematopoietic cell (right) with AP2A2-polarized clustering and asymmetric segregation into only one daughter cell (asterisk). Other daughter cell (no asterisk) reexpressed small vesicles of AP2A2 from time 3:58:04 onward (see also supplemental Videos 1-3). (C) HSC with diffuse, symmetric Ap2a2 distribution during and after mitosis with both daughter cells acquiring Ap2a2. (D) HSC with AP2A2 symmetric in division. Telophase midbody concentration is seen at time 2:39:42 (see also supplemental Videos 4-5). Videos were acquired with a DeltaVision video microscope fitted with a 37°C environmental chamber (Applied Precision) using Olympus 60×/1.42 numerical aperture oil-immersion lens and a Photometric CoolSnap HQ2 camera. Video analyses and still frames were performed with softWoRxExplorer Version 2.0 software (Applied Precision). All scale bars indicate 10 μm. (E-F) Influence of different feeder layers (external environment) on AP2A2 localization during mitosis. The terms symmetric and asymmetric were as defined in Figure 6E and I and C and F, respectively. D3-5 and D7-12 refer to days after CD150+48−KLS cell transduction with *Ap2a2*. NIH 3T3 (ie, GP+E-86) and OP9 are respective feeder layers. CK refers to cytokinesis seen (ie, a successful mitotic division). Failed M (mitosis)–apoptosis was defined as cells seen to be in mitosis for longer than 4 hours, because these cells would eventually abort mitosis to reenter interphase or undergo apoptosis. Analyses based on accumulated total number of dividing cells seen in each time period. (E) D3-5 with NIH 3T3 layer, total cells = 162 from 3 independent experiments; D7-12 with NIH 3T3 layer, total cells = 128 from 2 independent experiments. (F) D3-5 with OP9 layer, total cells = 147 from 2 independent experiments. All values presented are means ± SEM of respective experiment groups.

self-renewal capabilities within HSC populations has been reported previously.[37] Interestingly, the dormant fraction was seen to be 20%-30% of the total LT-HSC population,[26] which is similar to the percentage of ACDs seen in our in vitro videomicroscopy of *Ap2a2*-transduced HSCs. Our hypothesis of LT-HSC dormancy restricted to ACD is currently being addressed through postmitotic single-cell analyses.

In a parallel study to also identify novel HSC regulators, we performed and published an RNAi screen on a large cohort of our candidate polarity genes,[35] which included 3 shRNAs to *Ap2a2*. In the context of the current overexpression screen showing enhanced activity of *Ap2a2*-transduced HSCs, one might have expected impaired HSC repopulation with shRNA to *Ap2a2*. To try to understand why this was not the case for the 3 shRNAs to *Ap2a2* in our RNAi screen (http://www.bioinfo.iric.ca.self-renewal/), the initial caveat was that confirmation of specific gene knockdown was only performed retrospectively with the hairpins that provided impaired or enhanced HSC repopulation at the primary screen level. After screening, quantitative RT-PCR to assess Ap2a2 mRNA levels with the 1-, 2-, and 3-shAp2a2 hairpins showed that the maximal Ap2a2 knockdown was only 50% with 3-shAp2a2. Although the use of 4- and 5-shRNAs to Ap2a2 with greater knockdown also did not definitively show impairment of HSC reconstitution (supplemental Figure 2A-B), this has to be taken within the confines of our assay. For example, the RNAi screen identified Prkcz (also known as atypical protein kinase Cζ [aPKCζ]) as an enhancer of HSC activity, yet recent conditional aPKCζ studies demonstrated its dispensability in hematopoiesis.[47] Given that AP2A2 is part of the AP-2 heterotetrameric endocytic complex, with potential for redundancy from partners in the same complex, it might also require a conditional *Ap2a2* knock-out to see a hematopoiesis-specific phenotype.

In the setting of the crucial role of Ap2a2 in AP-2 clathrin-mediated endocytosis of transmembrane receptors, its overexpression in HSCs may either enhance or suppress the membrane expression of hematopoietic cytokine receptors known to be internalized via this endocytic pathway.[38] For example, thrombopoietin signaling is an important mediator of HSC quiescence,[39,40] and the thrombopoietin receptor is internalized via AP-2 endocytosis.[38] Because receptor internalization into endosomes form platform hubs of signaling,[41,42] Ap2a2-endosomes could involve the intersection of multiple signaling pathways such as tyrosine kinases and TGFβ- and G-coupled protein receptors. The in vitro effect of Ap2a2 overexpression on the HSCs could then result in either a niche-sensitized or niche-resistant HSCs that, after in vivo transplantation with subsequent asymmetric Ap2a2 segregation, would mediate differential composition or trafficking of signaling endosomes. In either case, Ap2a2-transduced HSCs seem to maintain a proliferative advantage.

Alternatively, the Ap2a2 endocytosis link may also function independently from cell signaling, because other essential cellular functions that can determine cell fate, such as cell cycle, apoptosis, and RNAi regulation, have been documented within the endocytic trafficking network.[41,43] The ability provided by observing asymmetric Ap2a2 segregation during HSC division delivers a unique opportunity to further investigate some of these aforementioned mechanisms.

Instinctively, the Ap2a2-Numb interaction would seem to be a key mechanism by which *Ap2a2* might influence HSC activity given the role of *Numb* as an inhibitor of Notch signaling. However, the disparity in localization of AP2A2 and NUMB is suggestive of differing and distinct mechanistic pathways for these 2 proteins in hematopoietic cell-fate decisions. In support of this is the absence of HSC phenotypes in the *Numb-Numblike* conditional mutant mouse[44] and in Notch-signaling mutant mice.[45,46] Whether

this phenomenon of AP2A2 and NUMB disparity is specific to primitive hematopoietic cells or if it occurs in other regenerative mammalian tissues remains to be explored. In addition, aPKCζ and aPKCλ, mammalian homologs of another classic invertebrate cell-fate determinant, aPKC, have been found to be dispensable for mammalian HSC activity,[47] supporting the idea that ACD in mammalian HSC self-renewal may involve as-yet-unidentified cell-fate determinants.

An important potential perspective relates to cancer, for which, apart from the possibility of tumors corrupting endosome signaling pathways for unrestrained growth,[48] there is significant accumulation of data from the *Drosophila* system linking perturbation of polarity and ACD at the stem-cell level to abnormal cell proliferation and cancer.[33,49] Moreover, there is a growing list of regulators of endocytosis that are aberrantly expressed in both human solid tissue and subtypes of hematologic cancers.[48] Two studies have reported that the balance between asymmetric versus symmetric divisions can be altered by, respectively, an oncogene (NUP98-HoxA9) in mammalian HSCs[18] and by a tumor suppressor (p53) in breast cancer stem cells,[34] with the implication that an underlying mechanism of both blood and solid-tissue cancers may be a perturbation of ACD. The fact that our mouse leukemias exhibited a symmetric pattern of Ap2a2 distribution potentially adds to these observations, and corruption of cell-fate mechanisms by cancer stem cells may become a critical tool used to fight oncogenesis.

Authorship

Contribution: S.B.T., E.D., and G.S. planned and performed the initial screen; S.B.T. performed all subsequent non-video experiments with significant contributions from E.D., K.H., S.C., J.C.,

N.M., M.H., and E.D.H.; S.B.T., J.F.D., and P.S.M. planned all videomicroscopy experiments; S.B.T. performed all videomicroscopy experiments; J.-P.L. constructed and maintains the IRIC self-renewal website; N.N.I. and laboratory staff performed all experiments and data analyses from cycling-quiescent microarrays; S.M.R. provided significant intellectual input; S.B.T and G.S. directed the research; S.B.T wrote the manuscript; and all authors read and approved the manuscript.

Conflict-of-interest disclosure: The authors declare no competing financial interests.

The current affiliation for S.B.T. is Stem Cell Research Group, Division of Blood Cancers, Australian Centre for Blood Diseases, Department of Hematology, Central Clinical School, Monash University-Alfred Health, Prahran, Australia. The current affiliation for K.H. is McMaster Stem Cell and Cancer Research Institute, McMaster University, Hamilton, ON.

Correspondence: Stephen B. Ting, Division of Blood Cancer, Australian Centre for Blood Diseases, Monash University–Alfred Health, The Alfred Centre, 99 Commercial Road, Melbourne, Victoria 3004, Australia; e-mail: stephen.ting@monash.edu.

References

1. Jan YN, Jan LY. Asymmetric cell division. *Nature.* 1998;392(6678):775-778.

2. Betschinger J, Knoblich JA. Dare to be different: asymmetric cell division in Drosophila, C. elegans and vertebrates. *Curr Biol.* 2004;14(16):R674-R685.

3. Knoblich JA. Mechanisms of asymmetric stem cell division. *Cell.* 2008;132(4):583-597.

4. Zhou Y, Atkins JB, Rompani SB, et al. The mammalian Golgi regulates numb signaling in asymmetric cell division by releasing ACBD3 during mitosis. *Cell.* 2007;129(1):163-178.

5. Coumailleau F, Furthauer M, Knoblich JA, Gonzalez-Gaitan M. Directional Delta and Notch trafficking in Sara endosomes during asymmetric cell division. *Nature.* 2009;458(7241):1051-1055.

6. Chia W, Somers WG, Wang H. Drosophila neuroblast asymmetric divisions: cell cycle regulators, asymmetric protein localization, and tumorigenesis. *J Cell Biol.* 2008;180(2):267-272.

7. Zhong W. Timing cell-fate determination during asymmetric cell divisions. *Curr Opin Neurobiol.* 2008;18(5):472-478.

8. Bowman SK, Neumuller RA, Novatchkova M, Du Q, Knoblich JA. The Drosophila NuMA Homolog Mud regulates spindle orientation in asymmetric cell division. *Dev Cell.* 2006;10(6):731-742.

9. Izumi Y, Ohta N, Hisata K, Raabe T, Matsuzaki F. Drosophila Pins-binding protein Mud regulates spindle-polarity coupling and centrosome organization. *Nat Cell Biol.* 2006;8(6):586-593.

10. Siller KH, Cabernard C, Doe CQ. The NuMA-related Mud protein binds Pins and regulates spindle orientation in Drosophila neuroblasts. *Nat Cell Biol.* 2006;8(6):594-600.

11. Suda J, Suda T, Ogawa M. Analysis of differentiation of mouse hemopoietic stem cells in culture by sequential replating of paired progenitors. *Blood.* 1984;64(2):393-399.

12. Giebel B, Zhang T, Beckmann J, et al. Primitive human hematopoietic cells give rise to differentially specified daughter cells upon their initial cell division. *Blood.* 2006;107(5):2146-2152.

13. Benveniste P, Cantin C, Hyam D, Iscove NN. Hematopoietic stem cells engraft with absolute efficiency. *Nat Immunol.* 2003;4(7):708-713.

14. Ema H, Sudo K, Seita J, et al. Quantification of self-renewal capacity in single hematopoietic stem cells from normal and Lnk-deficient mice. *Dev Cell.* 2005;8(6):907-914.

15. Dykstra B, Kent D, Bowie M, et al. Long-term propagation of distinct hematopoietic differentiation programs in vivo. *Cell Stem Cell.* 2007;1(2):218-229.

16. Beckmann J, Scheitza S, Wernet P, Fischer JC, Giebel B. Asymmetric cell division within the human hematopoietic stem and progenitor cell compartment: identification of asymmetrically segregating proteins. *Blood.* 2007;109(12):5494-5501.

17. Chang JT, Palanivel VR, Kinjyo I, et al. Asymmetric T lymphocyte division in the initiation of adaptive immune responses. *Science.* 2007; 315(5819):1687-1691.

18. Wu M, Kwon HY, Rattis F, et al. Imaging hematopoietic precursor division in real time. *Cell Stem Cell.* 2007;1(5):541-554.

19. Dykstra B, Ramunas J, Kent D, et al. High-resolution video monitoring of hematopoietic stem cells cultured in single-cell arrays identifies new features of self-renewal. *Proc Natl Acad Sci U S A.* 2006;103(21):8185-8190.

20. Deneault E, Cellot S, Faubert A, et al. A functional screen to identify novel effectors of hematopoietic stem cell activity. *Cell.* 2009;137(2):369-379.

21. Faubert A, Lessard J, Sauvageau G. Are genetic determinants of asymmetric stem cell division active in hematopoietic stem cells? *Oncogene.* 2004;23(43):7247-7255.

22. Sauvageau G, Thorsteinsdottir U, Eaves CJ, et al. Overexpression of HOXB4 in hematopoietic cells causes the selective expansion of more primitive populations in vitro and in vivo. *Genes Dev.* 1995;9(14):1753-1765.

23. Ohta H, Sekulovic S, Bakovic S, et al. Near-maximal expansions of hematopoietic stem cells in culture using NUP98-HOX fusions. *Exp Hematol.* 2007;35(5):817-830.

24. Antonchuk J, Sauvageau G, Humphries RK. HOXB4-induced expansion of adult hematopoietic stem cells ex vivo. *Cell.* 2002;109(1):39-45.

25. Cellot S, Krosl J, Chagraoui J, Meloche S, Humphries RK, Sauvageau G. Sustained in vitro trigger of self-renewal divisions in Hoxb4hiPbx1(10) hematopoietic stem cells. *Exp Hematol.* 2007;35(5):802-816.

26. Wilson A, Laurenti E, Oser G, et al. Hematopoietic stem cells reversibly switch from dormancy to self-renewal during homeostasis and repair. *Cell.* 2008;135(6):1118-1129.

27. Foudi A, Hochedlinger K, Van Buren D, et al. Analysis of histone 2B-GFP retention reveals slowly cycling hematopoietic stem cells. *Nat Biotechnol.* 2009;27(1):84-90.

28. Benveniste P, Frelin C, Janmohamed S, et al. Intermediate-term hematopoietic stem cells with extended but time-limited reconstitution potential. *Cell Stem Cell.* 2010;6(1):48-58.

29. Boehm M, Bonifacino JS. Adaptins: the final recount. *Mol Biol Cell.* 2001;12(10):2907-2920.

30. Rappoport JZ. Focusing on clathrin-mediated endocytosis. *Biochem J.* 2008;412(3):415-423.

31. Santolini E, Puri C, Salcini AE, et al. Numb is an endocytic protein. *J Cell Biol.* 2000;151(6):1345-1352.

32. Berdnik D, Torok T, Gonzalez-Gaitan M, Knoblich JA. The endocytic protein alpha-Adaptin is required for numb-mediated asymmetric cell division in Drosophila. *Dev Cell.* 2002;3(2):221-231.

33. Hawkins ED, Russell SM. Upsides and downsides to polarity and asymmetric cell division in leukemia. *Oncogene.* 2008;27(55):7003-7017.

34. Cicalese A, Bonizzi G, Pasi CE, et al. The Tumor Suppressor p53 Regulates Polarity of Self-Renewing Divisions in Mammary Stem Cells. *Cell.* 2009;138(6):1083-1095.

35. Hope KJ, Cellot S, Ting SB, et al. An RNAi screen identifies Msi2 and Prox1 as having opposite roles in the regulation of hematopoietic stem cell activity. *Cell Stem Cell.* 2010;7(1):101-113.

36. Ueno H, Sakita-Ishikawa M, Morikawa Y, Nakano T, Kitamura T, Saito M. A stromal cell-derived membrane protein that supports hematopoietic stem cells. *Nat Immunol.* 2003;4(5):457-463.

37. McKenzie JL, Gan OI, Doedens M, Wang JC, Dick JE. Individual stem cells with highly variable proliferation and self-renewal properties comprise the human hematopoietic stem cell compartment. *Nat Immunol.* 2006;7(11):1225-1233.

38. Hitchcock IS, Chen MM, King JR, Kaushansky K. YRRL motifs in the cytoplasmic domain of the thrombopoietin receptor regulate receptor internalization and degradation. *Blood.* 2008;112(6): 2222-2231.

39. Qian H, Buza-Vidas N, Hyland CD, et al. Critical role of thrombopoietin in maintaining adult quiescent hematopoietic stem cells. *Cell Stem Cell.* 2007;1(6):671-684.

40. Yoshihara H, Arai F, Hosokawa K, et al. Thrombopoietin/MPL signaling regulates hematopoietic stem cell quiescence and interaction with the osteoblastic niche. *Cell Stem Cell.* 2007;1(6):685-697.

41. Sorkin A, von Zastrow M. Endocytosis and signaling: intertwining molecular networks. *Nat Rev Mol Cell Biol.* 2009;10(9):609-622.

42. Gould GW, Lippincott-Schwartz J. New roles for endosomes: from vesicular carriers to multi-purpose platforms. *Nat Rev Mol Cell Biol.* 2009; 10(4):287-292.

43. Lee YS, Pressman S, Andress AP, et al. Silencing by small RNAs is linked to endosomal trafficking. *Nat Cell Biol.* 2009;11(9):1150-1156.

44. Wilson A, Ardiet DL, Saner C, et al. Normal hemopoiesis and lymphopoiesis in the combined absence of numb and numblike. *J Immunol.* 2007;178(11):6746-6751.

45. Mancini SJ, Mantei N, Dumortier A, Suter U, MacDonald HR, Radtke F. Jagged1-dependent Notch signaling is dispensable for hematopoietic stem cell self-renewal and differentiation. *Blood.* 2005;105(6):2340-2342.

46. Maillard I, Koch U, Dumortier A, et al. Canonical notch signaling is dispensable for the maintenance of adult hematopoietic stem cells. *Cell Stem Cell.* 2008;2(4):356-366.

47. Sengupta ADA, Ishikawa E, Florian MC, et al. Atypical protein kinase C (aPKCzeta and aPKCdelta) is dispensable for mammalian hematopoietic stem cell activity and blood formation. *Proc Natl Acad Sci U S A.* 2011;108(24):9957-9962.

48. Lanzetti L, Di Fiore PP. Endocytosis and cancer: an 'insider' network with dangerous liaisons. *Traffic.* 2008;9(12):2011-2021.

49. Coumailleau F, Gonzalez-Gaitan M. From endocytosis to tumors through asymmetric cell division of stem cells. *Curr Opin Cell Biol.* 2008;20(4):462-469.